Computers and Chemical Engineering 96 (2017) 69–74

Contents lists available at ScienceDirect

Computers and Chemical Engineering

journal homepage: www.elsevier.com/locate/compchemeng

Application of dodecahedron to describe the switching strategies of asynchronous simulated-moving-bed

Chuanyi Yao[a,*], Keju Jing[a], Xueping Ling[a], Yinghua Lu[a], Shaokun Tang[b]

[a] Department of Chemical and Biochemical Engineering, College of Chemistry and Chemical Engineering, Xiamen University, Xiamen, Fujian, 361005, China
[b] College of Chemical Engineering, Tianjin University, Tianjin, 300072, China

ARTICLE INFO

Article history:
Received 22 August 2016
Received in revised form 27 October 2016
Accepted 28 October 2016
Available online 3 November 2016

Keywords:
Asynchronous SMB
Dodecahedron
Visualization
Optimization
Separation techniques

ABSTRACT

Among various separation techniques, the simulated moving bed (SMB) process has received special attention, especially the asynchronous SMB that allocates the columns into four zones in a flexible way. With the relative switching times as variables in the Cartesian coordinates system, all applicable switching strategies in asynchronous SMB can be visualized in a dodecahedron with the initial configuration as the origin. Thus, any point in the dodecahedron represents a switching strategy, which could be easily obtained with initial configuration and coordinates. The dodecahedron includes 14 traditional SMB configurations, represented by the 14 vertexes of the dodecahedron. Based on the dodecahedron, the optimization of the asynchronous SMB was conducted through two case studies. Compared to traditional SMB, the feed flow rates were increased by 87% in the enantioseparation of 1,1′-bi-2-naphthol and 15% in the separation of glucose and fructose without the loss of product purities.

1. Introduction

Among various separation techniques, the simulated moving bed (SMB) process has attracted special attention in the past decades (Sa Gomes and Rodrigues, 2012). In the early stage, SMB was used in petroleum and sugar industries (Beste et al., 2000; Broughton, 1984; Lim, 2012; Ruthven and Ching, 1989). After its successful application in enantioseparation in 1990s, the application of SMB in pharmaceutical and fine chemical separation fields has been further explored (Negawa and Shoji, 1992; Rajendran et al., 2009) and nowadays it becomes a popular technique in bioseparation processes (Gueorguieva et al., 2011; Houwing et al., 2003; Li et al., 2007; Paredes et al., 2005; Wellhoefer et al., 2014; Xie et al., 2002).

In the traditional four zone SMB process, the four ports connecting desorbent, extract, feed and raffinate lines are switched at the same time. Hence, the four zones have fixed number of columns throughout the whole switching period. In 2000, Novasep changed the situation by proposing an asynchronous SMB known as Varicol, in which the inlet/outlet ports are shifted asynchronously (Ludemann-Hombourger et al., 2000). Due to different switching time for inlet/outlet ports, the number of columns in a zone may vary over time and hence the average number of columns can be a non-integer. Thus in Varicol, the allocation of the columns in the four zones is much more flexible. Varicol has been successfully applied in different separation systems, such as the chiral separation of 1,2,3,4-tetrahydro-1-naphthol (Ludemann-Hombourger et al., 2000), SB-553261 (Ludemann-Hombourger et al., 2002), propranolol (Toumi et al., 2003), pindolol (Zhang et al., 2007), mitotane (da Silva et al., 2012), and albendazole sulfoxide enantiomers (Lourenco et al., 2012). Moreover, it gives a higher productivity or lower desorbent consumption compared with traditional SMB (Ludemann-Hombourger et al., 2000, 2002; Toumi et al., 2003, 2002) especially when a low total number of columns is considered (Pais and Rodrigues, 2003).

However, a big challenge for asynchronous SMB is that its design and optimization becomes complicated due to the increased degree of freedom (Toumi et al., 2002; Yao et al., 2014). Though the equivalent true moving bed and the triangle theory, which are usually used to assist the design of traditional SMB (Biegler et al., 2005; Yao et al., 2014), in principle can be considered but they are not appropriate for the design of asynchronous SMB (Toumi et al., 2003). The first important decision in optimizing the asynchronous SMB process is to select the appropriate decision variables. Besides the flow rates Q_I–Q_{IV} and switching period t_s, the decision variables related to switching strategy include also the four switching times of the four ports (Toumi et al., 2002) and three average column length (Toumi et al., 2003). These two options have the discrepancy on

* Corresponding author.
E-mail address: cyao@xmu.edu.cn (C. Yao).

http://dx.doi.org/10.1016/j.compchemeng.2016.10.016
0098-1354/

how many variables that influence the system performance. This discrepancy was unified in our previous work (Yao et al., 2014), where the parallel shifting of switching times was proved to have no influence on system performance, in other words, only three of the four switching times of four ports influence the system performance independently. Based on this finding, we defined three new variables (relative switching times) to describe asynchronous SMB. By using the relative switching times, it is easy to transform the switching times to the average zone lengths or *vice versa*, and a systematic method for this kind of transformation was also developed. A preliminary optimization of operation conditions by using the relative switching times was already verified in our previous work (Yao et al., 2014), but the optimization method based on relative switching times needs to be further investigated.

In the present work, possible strategies to optimize asynchronous SMB have been completely explored and a dodecahedron is used to describe all the applicable optimization strategies for asynchronous SMB. The dodecahedron not only offers a concise graphical way for description of the strategies explored, but also simplifies the design and optimization of asynchronous SMB. The optimization based on the dodecahedron and relative switching times is further verified by two case studies for maximization of throughput.

2. Dodecahedron depicting the asynchronous SMB

The definitions in the previous work (Yao et al., 2014) are used here, for completion, they are summarized as follows:

$\boldsymbol{N}^0 = \left[N_{c,I}, N_{c,II}, N_{c,III}, N_{c,IV}\right]$, initial configuration, $N_{c,M}$ $(M = I, II, III, IV)$ is the number of columns in zone M.

$\bar{\boldsymbol{N}} = \left[\bar{N}_{c,I}, \bar{N}_{c,II}, \bar{N}_{c,III}, \bar{N}_{c,IV}\right]$, average configuration

$\boldsymbol{t} = [t_D, t_E, t_F, t_R]$, t_k $(k = D, E, F, R)$ is the switching time of k port

$\delta\boldsymbol{t}$=$[\delta t_D,\delta t_E,\delta t_F,\delta t_R]$=$[t_D,t_E,t_F,t_R]/t_s$, δt_k $(k = D, E, F, R)$ is the switching time of k port normalized to switching period (t_s). For Simple-Shifting-Scheme, each port shifts once in one switching period, so

$$0 \le \delta t_k \le 1 \tag{1}$$

The definition of the relative shifting time is given as: $\delta x = \delta t_E - \delta t_D$, $\delta y = \delta t_F - \delta t_E$, and $\delta z = \delta t_R - \delta t_F$. The difference between the switching times of any two ports should not be greater than t_s. This implies that the relative shifting time between any two ports should fall in the range of −1 to 1. The inequalities below explain this further:

$$-1 \le \delta x \le 1 \tag{2}$$

$$-1 \le \delta y \le 1 \tag{3}$$

$$-1 \le \delta z \le 1 \tag{4}$$

$$-1 \le \delta x + \delta y \le 1 \tag{5}$$

$$-1 \le \delta y + \delta z \le 1 \tag{6}$$

$$-1 \le \delta x + \delta y + \delta z \le 1 \tag{7}$$

By parallel shifting, we got $\delta\boldsymbol{t}_0$, = $\delta\boldsymbol{t} - \delta t_D$ = $[0,\delta x,\delta x + \delta y,\delta x + \delta y + \delta z]$ which is determined by only δx, δy, and δz.

Thus, the switching strategy in an asynchronous SMB is characterized by the initial configuration and relative shifting times. To facilitate understanding, they were taken as Cartesian coordinates. Using the initial configuration as origin, the space expanded by δx, δy, and δz is shown in Fig. 1. With the limitations of Eqs. (2)–(7), the rational space constructs a dodecahedron. All the 14 vertexes of this dodecahedron have integer coordinates and each of them corresponds to a traditional SMB configuration. As an example, when the initial configuration is 2/2/2/2, the coordinates and their corresponding traditional SMB configuration of the vertexes and origin are listed in Table 1.

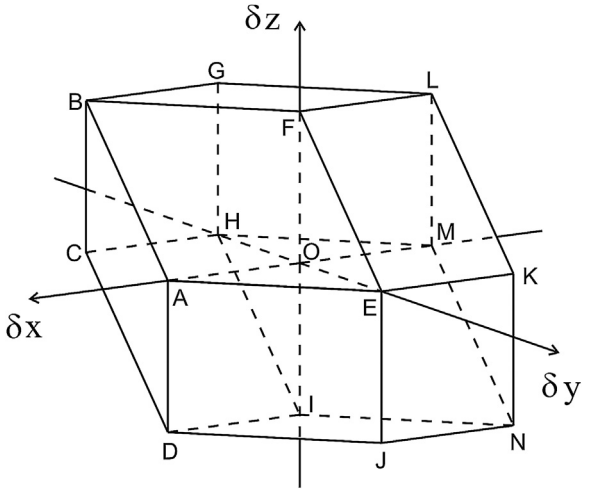

Fig 1. Dodecahedron: describing all the switching strategies of the asynchronous SMB process.

Table 1
Coordinates and corresponding traditional SMB configuration (SMB Conf.) of the origin and the vertexes of the dodecahedron.

Point	Coordinates	SMB conf.
O	(0, 0, 0)	2/2/2/2
A	(1, 0, 0)	1/2/2/3
B	(1, −1, 1)	1/3/1/3
C	(1, −1, 0)	1/3/2/2
D	(1, 0, −1)	1/2/3/2
E	(0, 1, 0)	2/1/2/3
F	(0, 0, 1)	2/2/1/3
G	(0, −1, 1)	2/3/1/2
H	(0, −1, 0)	2/3/2/1
I	(0, 0, −1)	2/2/3/1
J	(0, 1, −1)	2/1/3/2
K	(−1, 1, 0)	3/1/2/2
L	(−1, 0, 1)	3/2/1/2
M	(−1, 0, 0)	3/2/2/1
N	(−1, 1, −1)	3/1/3/1

The configuration of the corresponding coordinates in Table 1 could be easily obtained from the following correlation:

$$\bar{N}_{c,I} = N_{c,I} - \delta x \tag{8}$$

$$\bar{N}_{c,II} = N_{c,II} - \delta y \tag{9}$$

$$\bar{N}_{c,III} = N_{c,III} - \delta z \tag{10}$$

$$\bar{N}_{c,IV} = N_{c,IV} + \delta x + \delta y + \delta z \tag{11}$$

Actually, the configuration of any point (besides the vertexes) in the dodecahedron can be obtained with its coordinates and the initial configuration by using Eqs. (8)–(11), which are exactly the core of the systematic method for transformation between the average configuration and the switching strategy (Yao et al., 2014). For different initial configuration, Fig. 1 is identical besides the origin corresponding different initial configuration. This implies that the dodecahedron in Fig. 1 defines the optional space of switching strategy when designing or optimizing an asynchronous SMB process. Notably, the volume of the dodecahedron is only half of the circumscribed cube (i.e. $-1 \le \delta x, \delta y, \delta z \le 1$). Such smaller and more accurate searching space may enormously speed up the searching process. When the optimized point is obtained, $\boldsymbol{\delta t}_0$ can be organized with its definition and then, by parallel shifting, the switching strategy $\delta\boldsymbol{t}$ could be determined (Yao et al., 2014).

If the optimized point is too close to the border of the dodecahedron, it may indicate that the best operation point is located outside of the dodecahedron. Therefore, in this case, it is better to select another configuration as the origin and perform the optimization again. Actually, the closer the origin to the optimized point, the better the result. For a convenient view, the borders of the dodecahedron in all the 8 octants are listed below:

1st octant: $\delta x + \delta y + \delta z = 1$
2nd octant: $\delta x = -1, \delta y + \delta z = 1$
3rd octant: $\delta x + \delta y = -1, \delta z = 1$
4th octant: $\delta x = 1, \delta y = -1, \delta z = 1, \delta x + \delta y + \delta z = 1$
5th octant: $\delta x + \delta y = 1, \delta z = -1$
6th octant: $\delta x = -1, \delta y = 1, \delta z = -1, \delta x + \delta y + \delta z = -1$
7th octant: $\delta x + \delta y + \delta z = -1$
8th octant: $\delta x = 1, \delta y + \delta z = -1$

3. Mathematical model

For the simulations of asynchronous SMB process, we used the linear driving force (LDF) model, which was proved to be accurate and efficient (Biegler et al., 2005; Yao et al., 2013). The model equations for each column are as follows:

$$\frac{\partial c_i}{\partial t} + v\frac{\partial c_i}{\partial x} = D_a\frac{\partial^2 c_i}{\partial x^2} - \frac{1-\varepsilon_b}{\varepsilon_b}k_{e,i}\left(q_i^* - q_i\right) \tag{12}$$

$$\frac{\partial q_i}{\partial t} = k_{e,i}\left(q_i^* - q_i\right) \tag{13}$$

where c_i is the mobile-phase concentration of solute i, i =A (less retained component) or B (more retained component); q_i is the solid-phase concentration; q_i^* is the equilibrium concentration in the solid phase, which is governed by the adsorption isotherm with c_i; v is the interstitial velocity; D_a is the apparent dispersion coefficient; ε_b is the bed porosity; k_e is the effective mass transfer coefficient; x is the axial coordinates; t is the time. The model equations are solved by the space-time conservation element and solution element method (Lim et al., 2004; Lim and Jorgensen, 2004; Yao et al., 2014).

In the simulation of asynchronous SMB, the model equations were solved switch by switch. In each switch, the switching period was divided into several sub-intervals according to the switching strategy. At the end of the switching period, the state variables were used as the initial conditions for the next switch. This process was repeated until the cyclic steady state was reached (Minceva et al., 2003; Yao et al., 2013).

4. Optimization based on the dodecahedron

In this section, two case studies were used to demonstrate the optimization of the asynchronous SMB based on the dodecahedron. They are the enantioseparation of 1,1′-bi-2-naphthol (case 1) and glucose-fructose separation (case 2). The parameters of the two processes were obtained from the literature (Beste et al., 2000; Pais et al., 1997a,b, 1998) and they are listed in Table 2.

The equilibrium isotherms for the chiral separation process are as follows:

$$q_A^* = \frac{2.69c_A}{1 + 0.0336c_A + 0.0466c_B} + \frac{0.1c_A}{1 + c_A + 3c_B} \tag{14}$$

$$q_B^* = \frac{3.73c_B}{1 + 0.0336c_A + 0.0466c_B} + \frac{0.3c_B}{1 + c_A + 3c_B} \tag{15}$$

The isotherms for the sugar separation process are given by:

$$q_A^* = 0.32c_A + 0.000457c_Ac_B \tag{16}$$

$$q_B^* = 0.675c_B \tag{17}$$

4.1. Enantioseparation of 1,1′-bi-2-naphthol

The separation of 1,1′-bi-2-naphthol racemate has been optimized by SMB process (Pais et al., 1998) and the operation conditions obtained was a configuration of 2/2/2/2 (refer to Table 3). The experimental purities reached 93% for the extract (Pur_E) and 96.2% for the raffinate (Pur_R). Using asynchronous SMB, Wongso et al. (Wongso et al., 2005) studied this separation process and optimized the switching strategy and operation conditions to increase the feed flow rate (Q_F) without the loss of product purities.

In the present work, we dealt with the optimization of switching strategy and operation conditions for the enantioseparation of 1,1′-bi-2-naphthol based on the dodecahedron. In order to be certain that the product purities are not lower than the experimental values in literature (Pais et al., 1998), the penalty function method was introduced. Two parts of penalty were considered, PE (Pur_E) and PR (Pur_R):

$$PE = \begin{cases} 0, & \text{while} Pur_E \geq 0.93 \\ k|Pur_E - 0.93|, & \text{while} Pur_E < 0.93 \end{cases}$$

$$PR = \begin{cases} 0, & \text{while} Pur_R \geq 0.962 \\ k|Pur_R - 0.962|, & \text{while} Pur_R < 0.962 \end{cases}$$

where k is a large number, and 10^5 was used in this work.

So, the optimization problem becomes:

$\max Q_F - PE - PR\ (Q_E, Q_R, t_s, \delta x, \delta y, \delta z)$

subject to $-1 \leq \delta x, \delta y, \delta z, \delta x + \delta y, \delta y + \delta z, \delta x + \delta y + \delta z \leq 1$

The optimization was conducted by Box complex method and the results are listed in Table 3. The optimized point is located in the 6th octant, $\delta x + \delta y + \delta z = -0.31$, which is far away from the border ($\delta x + \delta y + \delta z = -1$).

As seen in Table 3, the feed flow rate in this work is much higher than previous works (Pais et al., 1997b, 1998; Wongso et al., 2005). Compared to traditional SMB process, it has increased by 87%. With respect to the optimized relative switching times, the switching strategy can easily be obtained as follows: $\boldsymbol{\delta t}_0 = \left[0, \delta x, \delta x + \delta y, \delta x + \delta y + \delta z\right] = [0, -0.32, 0.05, -0.31]$; $\delta \boldsymbol{t} = \delta \boldsymbol{t}_0 + 0.95 = [0.95, 0.63, 1, 0.64]$.

For comparison, the optimized switching strategies from Wongso et al. (Scheme 1) and this work (Scheme 2) are shown in Fig. 2. In Scheme 1, the switching period was divided into 4 equal sub-intervals, so the number of columns in each zone must be multiples of 1/4. In Scheme 2, the allocation of columns in the four zones was divided unequally, with the switching times at $0.63t_s$, $0.64t_s$, $0.95t_s$ and t_s. Thus, Scheme 2 is much more flexible. Moreover, we believe it is among the best strategy of the asynchronous SMB since all the possibilities were fully explored by the optimization method based on the dodecahedron. Notably, the robustness of the optimized point (i.e. the operation conditions listed in Table 3) is not satisfactory, the perturbation of operation conditions may lead to the decrease of product purities. Such as when the feed flow rate increased by 0.5 mL min^{-1}, the purity of raffinate is decreased to 93.86% with the purity of the extract is not significantly influenced. Thus, for robust operation, a more "conservative" operation condition is preferable. Based on optimization, it is found that the operation conditions of Q_I = 56.83 mL min^{-1}, Q_E = 19.67 mL min^{-1}, Q_F = 6.10 mL min^{-1}, Q_R = 11.29 mL min^{-1} and t_s = 2.89 min for Scheme 2 can guarantee the product purities fulfill the requirement of PurE ≥ 93% and PurR ≥ 96.2% in the range of feed flow rate 6.10 ± 0.5 mL min^{-1}.

Meanwhile, marked by dashed lines in Fig. 2, Scheme 2 contains 4 switches in one switching period, i.e. one switch is for one port. Such strategy was defined previously and was called simple-shifting-scheme, which gives the best performance for a certain

Table 2
Parameters of enantioseparation of 1,1′-bi-2-naphthol (case 1) and glucose-fructose separation (case 2).

Item	Case 1	Case 2
Column	i.d. 2.6 cm × 10.5 cm	i.d. 2.6 cm × 52.07 cm
Total number of columns	8	8
Bed porosity	0.4	0.41
Dispersion coefficient, $cm^2\ min^{-1}$	$10.5 \times 10^{-3}v$	$0.153v$
Mass transfer coefficient, min^{-1}	$k_{e,A} = k_{e,B} = 6.0$	$k_{e,A} = 0.9$, $k_{e,B} = 0.72$
Feed concentration, $g\ L^{-1}$	$c_A = c_B = 2.9$	$c_A = 322$, $c_B = 363$

Table 3
Performance of the enantioseparation of 1,1′-bi-2-naphthol with different optimized strategies for maximum feed flow rate.

	SMB, Pais et al. (1998)	Asynchronous SMB	
		Wongso et al. (2005)	this work
Q_I/mL min^{-1}	56.83	56.83	56.83
Q_D/mL min^{-1}	21.45	21.45	21.45
Q_E/mL min^{-1}	16	18.49	18.93
Q_R/mL min^{-1}	9.09	6.65	9.34
Q_F/mL min^{-1}	3.64	3.69 (+1.4%)	6.82 (+87.4%)
t_s/min	2.75	2.96	2.81
δx, δy, δz	–	–	−0.32, 0.37, −0.36
configuration	2/2/2/2	1.25/2.5/2.25/2	2.32/1.63/2.36/1.69
PurE/%	93	93.05	93
PurR/%	96.2	96.39	96.2

Table 4
Performance of the sugar separation process by traditional and asynchronous SMB optimized for maximum feed flow rate.

	SMB, (Beste et al., 2000)	Asynchronous SMB, this work
Q_I/mL min^{-1}	15.89	15.89
Q_{II}/mL min^{-1}	11.0	11.40
Q_{III}/mL min^{-1}	12.67	13.32
Q_{IV}/mL min^{-1}	9.1	8.55
Q_F/mL min^{-1}	1.67	1.92 (+15%)
t_s/min	16.39	15.90
δx, δy, δz	–	0.06, −0.54, 0.39
configuration	2/2/2/2	1.94/2.54/2.61/0.91
PurE/%	90.2	90.2
PurR/%	96.6	96.6

average configuration (Yao et al., 2014). For the average configuration in Scheme 1, i.e. $\bar{\boldsymbol{N}} = [1.25, 2.5, 2.25, 2]$, a better performance could be reached by a simple-shifting-scheme of $\delta\boldsymbol{t} = [1, 0.75, 0.25, 1]$ if $\boldsymbol{N}^0 = [1, 2, 3, 2]$ is selected as the initial configuration.

To compare the concentrations and purities of the products extracted using asynchronous and traditional SMB, the internal concentration profiles of Scheme 2 and traditional SMB at half of switching period were calculated. As shown in Fig. 3, the concentration of less retained component in zone III in asynchronous SMB process is much higher than that in traditional SMB. Similarly, the more retained component is much more concentrated in Zone II. Thus, Scheme 2 has a higher product concentration. In addition, by comparing the concentrations between the less retained component and the more retained component, the purities of the products obtained using two strategies are roughly the same. Notably, in asynchronous SMB (Scheme 2), the extract and raffinate ports are corresponding to the column number 2.32 and 6.31 (Fig. 3), whereas in traditional SMB, the extract and raffinate are withdrawn at the ends of column 2 and column 6.

Importantly, in Scheme 2 the desorbent port was switched at $0.95t_s$. Generally, a switching period begins after the switching of desorbent port. Since simple shifting scheme is not unique and can be modified by parallel shifting without influencing the performance (Yao et al., 2014). We can get another switching strategy (Scheme 3 in Fig. 2), where the switching period begins after the switch of desorbent port. In the $\delta x - \delta y - \delta z$ space, Scheme 2 corresponds to a point, P1 (−0.32, 0.37, −0.36), in the dodecahedron with 2/2/2/2 as origin (refer to Fig. 1). Different from Scheme 2, Scheme 3 is located in another dodecahedron with 2/1/3/2 (point J in Fig. 1) as origin. With $\boldsymbol{N}^0 = [2, 1, 3, 2]$ and $\bar{\boldsymbol{N}} = [2.32, 1.63, 2.36, 1.69]$, the coordinates of the point (P2) for Scheme 3 was easily calculated as: $\delta x = -0.32$, $\delta y = -0.63$, $\delta z = 0.64$. Under a coordinate translation, it can be seen that P2 is exactly the same point as P1. This is the advantage of the optimization method described in this work: numerous switching strategies that are differing in parallel shifting result in the same performance. Graphically, all the points representing these switching strategies are the same points under a coordinate translation in the $\delta x - \delta y - \delta z$ space.

4.2. Sugar separation process

The glucose-fructose separation has been optimized using traditional SMB (Beste et al., 2000). With a configuration of 2/2/2/2, the experimental purities were $Pur_E = 90.2\%$ and $Pur_R = 96.6\%$. In the present work, the asynchronous SMB process was investigated to improve the throughput. To ensure the system pressure within the allowable value, Q_I was fixed to the same as the experimental value in the work of Beste et al. (Beste et al., 2000). Thus, the decision variables include Q_{II}, Q_{III}, Q_{IV}, t_s, δx, δy, and δz. Similarly to the case study in Section 4.1, the penalty function method was used to ensure that the product purities are not lower than the experimental values in SMB (refer to Table 4). The optimization problem is described as follows.

$$\max\ Q_F - PE - PR\ (Q_{II}, Q_{III}, Q_{IV}, t_s, \delta x, \delta y, \delta z)$$

$$\text{subject to } -1 \le \delta x, \delta y, \delta z, \delta x + \delta y, \delta y + \delta z, \delta x + \delta y + \delta z \le 1 \text{where,}$$

$$PE = \begin{cases} 0, & \text{while} Pur_E \ge 0.902 \\ k|Pur_E - 0.902|, & \text{while} Pur_E < 0.902 \end{cases}$$

$$PR = \begin{cases} 0, & \text{while} Pur_R \ge 0.966 \\ k|Pur_R - 0.966|, & \text{while} Pur_R < 0.966 \end{cases}$$

First we used the configuration 2/2/2/2 as the initial configuration, i.e. the origin in the dodecahedron, to obtain the optimized point, called P_I, with the coordinates of $\delta x = 0.04$, $\delta y = -0.48$, and $\delta z = -0.52$. Of note, P_I is located in the eighth octant of Fig. 1 and exactly at the border ($\delta y + \delta z = -1$), indicating that the best point exists outside of this dodecahedron. Accordingly, the optimization

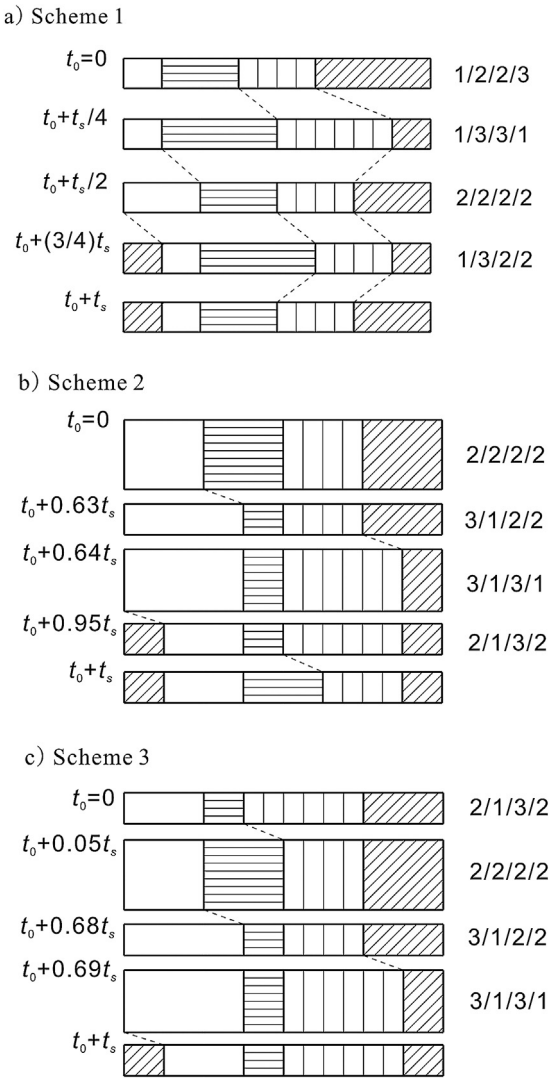

Fig. 2. Switching strategies for enantioseparation of 1,1′-bi-2-naphthol racemate by the asynchronous SMB. a) optimized result from Wongso et al.[25] b) & c) two equivalent optimized switching strategies obtained in this work. Switches are marked by dashed lines.

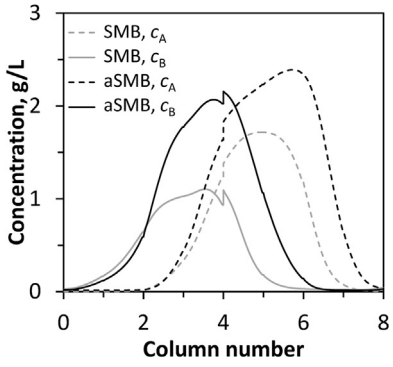

Fig. 3. Internal concentration profiles in traditional SMB and asynchronous SMB (aSMB) at $t = t_0 + 0.5t_s$ when cyclic steady state is achieved. t_0 is the time according to the port switch associated with desorbent line. c_A, less retained component; c_B, more retained component.

Fig. 4. Optimized switching strategy in the asynchronous SMB process for separation of glucose and fructose based on dodecahedron.

was conducted again in another dodecahedron with point I in Fig. 1 (i.e. configuration of 2/2/3/1) as the origin and the optimized point (P_{II}) was located in the fourth octant, which is far away from the border. The optimized results are summarized in Table 4.

It can be seen in Table 4 that asynchronous shifting increases the feed flow rate by 15% without the loss of product purities. With the coordinates of P_{II}, the switching strategy was obtained as: $\boldsymbol{\delta t}_0 = [0, \delta x,\ \delta x + \delta y,\ \delta x + \delta y + \delta z] = [0, 0.06,\ -0.48,\ -0.09]$; $\delta \boldsymbol{t} = \delta \boldsymbol{t_0} + 0.94 = [0.94, 1, 0.46, 0.85]$. The switching strategy is shown in Fig. 4.

Notably, Zone IV disappears from $0.85t_s$ to $0.94t_s$, which is feasible in the asynchronous SMB process. Considering the actual number of columns in zone M (M = I, II, III, IV) in the simple-shifting-scheme can only change between floor($\tilde{N}_{c,M}$) and ceil($\tilde{N}_{c,M}$), where floor($\tilde{N}_{c,M}$) and ceil($\tilde{N}_{c,M}$) are the nearest integers lower and higher than $\tilde{N}_{c,M}$ (Yao et al., 2014). So as long as the average number of columns in a zone is larger than 1, this zone remains throughout the entire switching period. On the other hand, if the average number of columns in any zone is less than 1, this zone will disappear for a certain time in a switching period.

5. Conclusions

In the present work we used a dodecahedron to describe the switching strategies of the asynchronous SMB. The relative switching times were taken as the three variables of the Cartesian coordinates and the initial configuration was regarded as the origin. The dodecahedron covers all the configurations applicable for the asynchronous SMB, including traditional SMB represented by the 14 vertexes of the dodecahedron. Every point in the dodecahedron could be easily converted to the average configuration in the switching strategies.

Not only did the dodecahedron provide a visualized description of the asynchronous SMB process, but it also simplified the optimization and design of the switching strategy for the asynchronous SMB. Based on the dodecahedron, the optimization of asynchronous SMB was demonstrated in two cases. In the enantioseparation of 1,1′-bi-2-naphthol, the feed flow rate was increased by 87% with the optimized asynchronous switching strategy, without the loss of product purities and additional investment. In the separation of glucose and fructose, compared to the traditional SMB, the feed flow rate under the optimized asynchronous SMB was increased by 15%.

Acknowledgements

This work was supported by the National Natural Science Foundation of China (No. 21206118), the Fundamental Research Funds for the Central Universities (No. 2010121049) and the Science and Technology Program of Xiamen (No. 3502Z20143008)

References

Beste, Y.A., Lisso, M., Wozny, G., Arlt, W., 2000. Optimization of simulated moving bed plants with low efficient stationary phases: separation of fructose and glucose. J. Chromatogr. A 868, 169–188.

Biegler, L.T., Jiang, L., Fox, V.G., 2005. Recent advances in simulation and optimal design of pressure swing adsorption systems. Sep. Purif. Rev. 33, 1–39.

Broughton, D.B., 1984. Production-scale adsorptive separations of liquid mixtures by simulated moving-bed technology. Sep. Sci. Technol. 19, 723–736.

Gueorguieva, L., Palani, S., Rinas, U., Jayaraman, G., Seidel-Morgenstern, A., 2011. Recombinant protein purification using gradient assisted simulated moving bed hydrophobic interaction chromatograph. Part II: process design and experimental validationy. J. Chromatogr. A 1218, 6402–6411.

Houwing, J., Billiet, H.A.H., van der Wielen, L.A.M., 2003. Mass-transfer effects during separation of proteins in SMB by size exclusion. AlChE J. 49, 1158–1167.

Li, P., Xiu, G., Rodrigues, A.E., 2007. Proteins separation and purification by salt gradient ion-exchange SMB. AlChE J. 53, 2419–2431.

Lim, Y.I., Jorgensen, S.B., 2004. A fast and accurate numerical method for solving simulated moving bed (SMB) chromatographic separation problems. Chem. Eng. Sci. 59, 1931–1947.

Lim, Y.I., Chang, S.C., Jorgensen, S.B., 2004. A novel partial differential algebraic equation (PDAE) solver: iterative space-time conservation element/solution element (CE/SE) method. Comput. Chem. Eng. 28, 1309–1324.

Lim, Y.I., 2012. Optimal flushing flow rates in para-xylene simulated moving-bed considering geometric factor of dead volume. Adsorption 18, 469–482.

Lourenco, T.C., Batista Jr, J.M., Furlan, M., He, Y., Nafie, L.A., Santana, C.C., Cass, Q.B., 2012. Albendazole sulfoxide enantiomers: preparative chiral separation and absolute stereochemistry. J. Chromatogr. A 1230, 61–65.

Ludemann-Hombourger, O., Nicoud, R.M., Bailly, M., 2000. The VARICOL process: a new multicolumn continuous chromatographic process. Sep. Sci. Technol. 35, 1829–1862.

Ludemann-Hombourger, O., Pigorini, G., Nicoud, R.M., Ross, D.S., Terfloth, G., 2002. Application of the VARICOL process to the separation of the isomers of the SB-553261 racemate. J. Chromatogr. A 947, 59–68.

Minceva, M., Pais, L.S., Rodrigues, A.E., 2003. Cyclic steady state of simulated moving bed processes for enantiomers separation. Chem. Eng. Process. 42, 93–104.

Negawa, M., Shoji, F., 1992. Optical resolution by simulated moving-bed adsorption technology. J. Chromatogr. A 590, 113–117.

Pais, L.S., Rodrigues, A.E., 2003. Design of simulated moving bed and Varicol processes for preparative separations with a low number of columns. J. Chromatogr. A 1006, 33–44.

Pais, L.S., Loureiro, J.M., Rodrigues, A.E., 1997a. Modeling simulation and operation of a simulated moving bed for continuous chromatographic separation of 1, 1'-bi-2-naphthol enantiomers. J. Chromatogr. A 769, 25–35.

Pais, L.S., Loureiro, J.M., Rodrigues, A.E., 1997b. Separation of 1,1'-bi-2-naphthol enantiomers by continuous chromatography in simulated moving bed. Chem. Eng. Sci. 52, 245–257.

Pais, L.S., Loureiro, J.M., Rodrigues, A.E., 1998. Modeling strategies for enantiomers separation by SMB chromatography. AlChE J. 44, 561–569.

Paredes, G., Makart, S., Stadler, J., Mazzotti, M., 2005. Simulated moving bed operation for size exclusion plasmid purification. Chem. Eng. Technol. 28, 1335–1345.

Rajendran, A., Paredes, G., Mazzotti, M., 2009. Simulated moving bed chromatography for the separation of enantiomers. J. Chromatogr. A 1216, 709–738.

Ruthven, D.M., Ching, C.B., 1989. Counter-current and simulated counter-current adsorption separation processes. Chem. Eng. Sci. 44, 1011–1038.

Sa Gomes, P., Rodrigues, A.E., 2012. Simulated moving bed chromatography: from concept to proof-of-concept. Chem. Eng. Technol. 35, 17–34.

Toumi, A., Hanisch, F., Engell, S., 2002. Optimal operation of continuous chromatographic processes: mathematical optimization of the VARICOL process. Ind. Eng. Chem. Res. 41, 4328–4337.

Toumi, A., Engell, S., Ludemann-Hombourger, O., Nicoud, R.M., Bailly, M., 2003. Optimization of simulated moving bed and Varicol processes. J. Chromatogr. A 1006, 15–31.

Wellhoefer, M., Sprinzl, W., Hahn, R., Jungbauer, A., 2014. Continuous processing of recombinant proteins: integration of refolding and purification using simulated moving bed size-exclusion chromatography with buffer recycling. J. Chromatogr. A 1337, 48–56.

Wongso, F., Hidajat, K., Ray, A.K., 2005. Improved performance for continuous separation of 1,1'-bi-2-naphthol racemate based on simulated moving bed technology. Sep. Purif. Technol. 46, 168–191.

Xie, Y., Mun, S., Kim, J., Wang, N.H.L., 2002. Standing wave design and experimental validation of a tandem simulated moving bed process for insulin purification. Biotechnol. Progr. 18, 1332–1344.

Yao, C., Tang, S., Yao, H.M., Tade, M.O., 2013. Continuous prediction technique for fast determination of cyclic steady state in simulated moving bed process. Comput. Chem. Eng. 58, 298–304.

Yao, C., Tang, S., Yao, H.-M., Tade, M.O., Xu, Y., 2014. Study on the number of decision variables in design and optimization of Varicol process. Comput. Chem. Eng. 68, 114–122.

Zhang, Y., Hidajat, K., Ray, A.K., 2007. Enantio-separation of racemic pindolol on −acid glycoprotein chiral stationary phase by SMB and Varicol. Chem. Eng. Sci. 62, 1364–1375.

da Silva, A.C., Salles, A.G., Perna, R.F., Correia, C.R.D., Santana, C.C., 2012. Chromatographic separation and purification of mitotane racemate in a Varicol multicolumn continuous process. Chem. Eng. Technol. 35, 83–90.